VOL. 05 NO. 5,
AUGUST, 2024
E-ISSN 3027-1339
P-ISSN 3026-8257

African Scholar Publications & Research International
www.africanscholarpub.com

Journal of Systematic, Evaluation and Diversity Engr. (JSEDE)

Using Neural Networks Based Devices to Reduce Power Loss in the Nigerian Transmission Line Network

Orji Ude O.[1]; & Madueme Theophilus C.[2]
[1]Department of Electrical/Electronic Engineering, Abia State Polytechnic, Aba
[2]Department of Electrical Engineering, Faculty of Engineering, University of Nigeria, Nsukka, Nigeria.
Corresponding Author: *orjivic2005@yahoo.com*

Abstract
Three necessary analyses were carried out on the Nigerian 330 kV power transmission network that consists of 14 generators, 59 buses, 39 load points and 111 transmission lines. These analyses viz; eigenvalue, participation factor and damping ratio, were carried out to obtain buses that contributed to the stability of the network. The network was modelled with MATLAB Simulink. The load bus Eket TS was stable during the analyses and selected as the best location for the simulation of Unified power flow controller (UPFC). The load, on the bus, was varied using a 50% increment (198 MW, 297 MW, 396 MW, 495 MW, and 594 MW). The performance of the proposed system was compared with Thyristor Controlled Series Capacitor (TCSC). The active power loss in the system was reduced by 7.965% with TCSC and 14.04% with UPFC. For the reactive power loss, the TCSC reduced the reactive loss by 8.255%; UPFC reduced the reactive loss by 24.67%. The UPFC outperformed the TCSC by 6.08% in reducing active power losses and by 15.345% in reducing reactive power losses. The neural network-controlled UPFC achieved a better loss reduction than the TCSC.

Keywords: UPFC, TCSC, Eigenvalue, Participation Factor, Damping Ratio

Introduction
Electrical energy is transmitted via transmission lines that run from one place to another. As a result of the physical properties of the transmission medium, transmission line losses are inevitable. Generation Companies (GENCOs) site their plants near generation resources and transmission lines for easy evacuation.

These factors conspire to limit power generation to the southern part of the country. These are evident in the siting bulk of the power generation facilities in the Southern part of Nigeria, from where power is transmitted to distant parts of the grid [1]. The overall effect is the reduced quantity of transmitted power and the uneven load distribution on the network. It becomes difficult to maintain power system security and reliability.Adequate measures must be put in place to reduce power losses. Ideally, losses in an electric system should be around 3% - 6% however, developing countries experience active power losses is about 20% [2]. In the power system, engineers and researchers are constantly in search of ways to reduce reactive power and transmission loss to boost system efficiency. As the transmission line losses reduce, the active power delivered will increase [3].Flexible AC Transmission Systems (FACTS) devices are recently well-known for higher controllability in power systems utilizing power electronic devices [4]. They are effective alternatives for power systems performance improvements like voltage security, transfer capability and loss reduction [5]. The application of FACTS devices in power systems improvement was studied using the Nigerian power network. The maximum power transmission capacity of the Nigerian 330 kV network was improved using the FACTS device [6]. Active power losses, system operating costs and congestion in the power systems network were reduced with FACTS devices modelled on IEEE-30 and IEEE-57 bus systems [7]. FACTS devices improved power flow by reducing fault current modelled on an IEEE 9-BUS 3 machine system [8]. Differential Evolution (DE) application optimally allocated FACTS devices on an IEEE 30-bus test system to reduce power losses and improve the voltage profile [9]. This study aims to minimize power losses in transmission networks with FACTS devices. The objective was to model UPFC for optimal power loss minimization on the Nigerian 330kV power transmission system.

OVERVIEW OF FACTS DEVICES

In general, FACTS controllers can be divided into four categories [10]

i. Series controllers
ii. Shunt controllers
iii. Combined series-series controllers
iv. Combined series-shunt controllers

Series Controllers

The series controller could be a variable impedance, such as a capacitor, reactor, etc., or anelectronics-based based variable source of frequency, sub-synchronous and harmonic frequencies (or a combination) to serve the desired need. In principle, all series controllers inject voltage in series with the line. As long as the voltage is in phase quadrature with the line current, the series controller only supplies or consumes

variable reactive power. Any other phase relationship will be in the handling of real power as well. Series controllers include SSSC, IPFC, TCSC, TSSC, TCSR, and TSSR.

Shunt Controllers

The shunt controllers may be variable impedance, variable source, or a combination of both. In principle, all shunt controllers inject current into the system at the point of connection. Even a shunt impedance connected to the line voltage causes a variable current flow representing the injection of current into the line. As long as the injected current is in phase quadrature with line voltage, the shunt controller only supplies or consumes variable, reactive power. Any other phase relationship will involve the handling of real power as well. Shunt controllers include STATCOM, TCR, TSR, TSC, and TCBR.

Combined Series-Series Controllers

This is a combination of separate series controllers controlled in a coordinated manner by a multiline transmission system or unified controller. The controllers in series provide independent series reactive compensation for each line and transfer real power via the power link. The active power transfer capability of the unified series-series controller, interline power flow controller, makes it possible to balance both the active and reactive power flow in the lines and thereby maximize the utilization of the transmission system. Note that unified means that the dc terminals of all controllers are connected for power transfer.

Combined Series-Shunt Controllers

It is a combination of separate shunt and series controllers controlled in a coordinated manner by a Unified Power Flow Controller with series and shunt elements. In principle, combined shunt and series controllers inject current into the system with the shunt part of the controller and voltage in series with the line. A unified shunt and series controller allows exchange between the series and shunt controllers via a power link. Combined series-shunt controllers include UPFC, TCPST and TCPAR.

ARTIFICIAL NEURAL NETWORK

Artificial neural networks (ANNs) have become popular and helpful models for classification, clustering, pattern recognition and prediction in power systems investigation [11, 12]. The applications of ANNs can be seen in the data analysis, especially when factors such as accuracy, processing speed, latency, performance, fault tolerance, volume, scalability and convergence are of the essence [13]. Artificial neural networks investigate the effect of contingencies on power system security and

predict the critical contingencies that can violate the operational limits of a power system network [14, 15]. Artificial neural networks handle contingency ranking or screening under online monitoring with less computational time [16, 17].

STABILITY ASSESSMENT OF POWER SYSTEMS NETWORK BEFORE THE INSTALLATION OF FACTS DEVICES

System stability assessment must precede the installation of FACTS devices [18, 19]. Several approaches to the stability study of such a system are based on the transfer function, state-space modelling and small-signal analysis based on the linearization around an operating point and calculating the eigenvalues, nonlinear method, and the impedance-based method [20, 21]. The nonlinear methods have computational complexity and become difficult to study complex power systems networks with power electronic devices. The impedance and eigenvalue-based analyses need less computation and include the impact of controller dynamics and the grid impedance [22, 23]; the eigenvalue-based approach is a global stability analysis method that determines the system status, regardless of the location of the source of instability [24]. The eigenvalue-based analysis has broad usage in determining the stability status of a wind turbine system, harmonic stability assessment, and stability of two-terminal and multi-terminal Voltage Source Converter (VSC) and Modular Multi-level Converter-based HVDC transmission systems [20, 25]. Also, the participation factor analysis and the damping ratio detect buses with high contribution to harmonic instability excitation. Such instability problems affect the overall stability status of the system [26, 27].

METHODOLOGY

Three vital analyses viz: eigenvalue analysis, participation factor analysis and damping ration analysis were carried out on the Nigerian 330kV power transmission network using MATLAB Simulink. The outcomes of these analyses were pivotal in determining the load bus stable for the installation of Neural Network controlled UPFC during load variation. The Unified Power Flow Controller (UPFC) reduced the power losses in the Nigerian 330kV power system. The UPFC was controlled with Artificial Neural Network to minimize power flow losses. The UPFC was placed in the network to control the system current flow and voltage optimally and reduce losses in the power system. The Nigerian 330kV power system model in MATLAB Simulink was used to evaluate the performance of the neural network-based UPFC.The power system network performance with neural network-controlled UPFC was compared with Thyristor Controlled Series Capacitor.

UPFC MODEL WITH NEURAL NETWORK

The Schematic diagram of the power circuit of a UPFC is given in Figure 1.

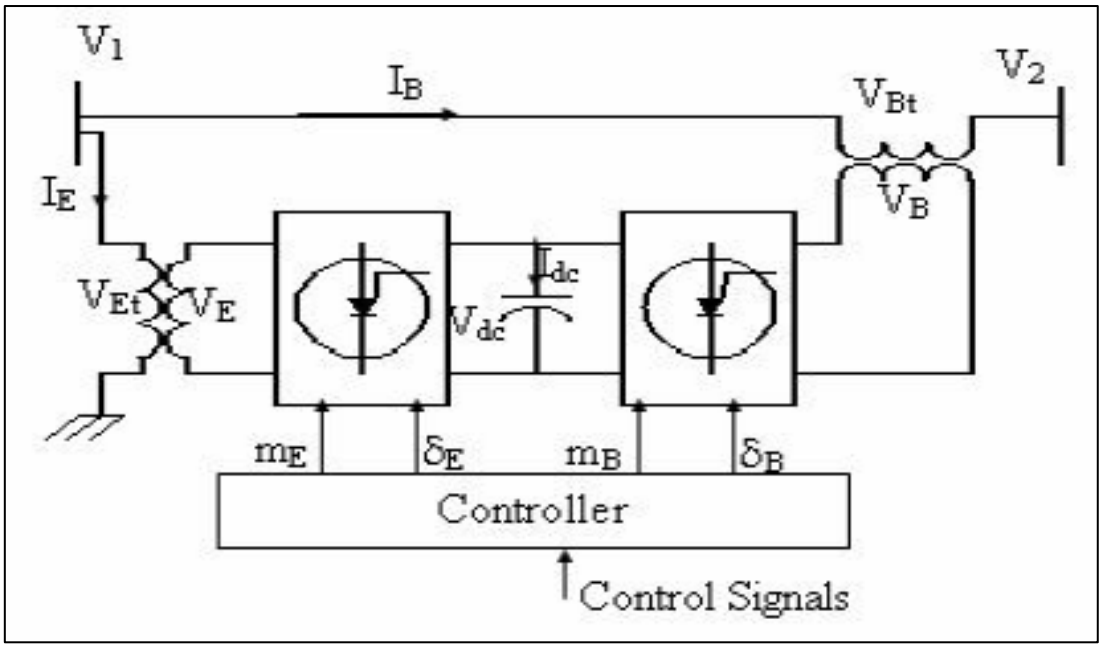


Figure 1: Schematic diagram of the power circuit of a UPFC [28]

The equations representing the UPFC model with its control input are thus;

$$\frac{di_E}{dt} = \frac{-r_E}{I_E} i_E + \frac{1}{I_E} V_{Et} - \frac{1}{I_E} V_E \quad 1$$

$$\frac{di_E}{dt} = \frac{-r_E}{I_E} i_E + \frac{1}{I_E} V_{Et} - \frac{1}{I_E} V_E \quad 2$$

$$V_E = \frac{\sqrt{2} m_E V_{dc}}{2} \cos(\omega t + \delta_E) \quad 3$$

$$V_B = \frac{\sqrt{2} m_B V_{dc}}{2} \cos(\omega t + \delta_B) \quad 4$$

m_B and m_E are control inputs representing the amplitude modulation ratioand δ_B are controlputs representing the phase angle of the control signal.

The phasor quantity for V_E and V_B is given thus;

$$V_E = \frac{m_E V_{dc}}{2} \angle \delta_E \quad 5$$

$$V_B = \frac{m_B V_{dc}}{2} \angle \delta_B \quad 6$$

$$\frac{dV_{dc}}{dt} = \frac{m_E}{2C_{dc}} \cos(\omega t + \delta_E) i_E + \frac{m_B}{2C_{dc}} \cos(\omega t + \delta_B) i_B \quad 7$$

The shunt series controllers of the UPFC control the reactive power injection or absorption from the power system. The neural network determines the levels of amplitude modulation ratios (m_E,m_B) and phase angles (i.e firing angles δ_E, δ_B,) of the control signal of each VSC in the UPFC. Two neural network controllers were used to control the injection of real and reactive power: One for the control of the series VSCcontrolling the series VSC and the other for controlling the shunt controller. The Neural Network-based UPFC is a multi-layer Network-based network model that is trained with a Modified Recursive Prediction Error Algorithm (MRPE). Figure 2 describes the model.

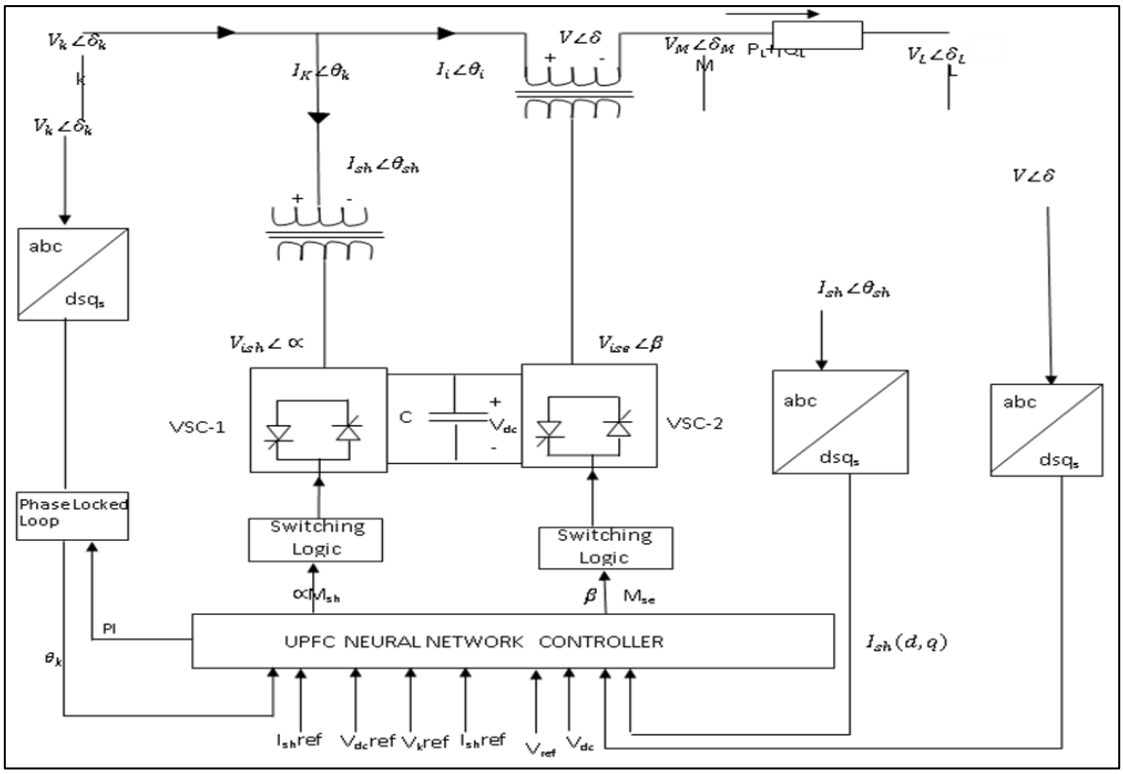


Figure 2: The UPFC Model [10]

The neural network controls the injection of real and reactive power by the UPFC into the transmission line such that the power losses are minimized. The main objective of the series converter is to produce an ac voltage of controllable magnitude and phase angle, and inject this voltage at fundamental frequency into the transmission line, exchanging real and reactive power. The series-connected controller required real power at the dc terminals; thus, real power flows between the controller shunt and series ac terminals through the common dc link.

The θk input is produced by the phase-locked loop as shown in figure 2. The phase-locked loop (PLL) is a feedback control system. This work is implemented with MATLAB Simulink. The phase-locked loop is a fundamental positive sequence component of the system voltage which synchronizes the AC output voltage of the VSCs. In the input to the PLL is the direct-quadrature-zero transform of the bus k voltage phase-locked this is done to transform the three-phase signal to the dq0 rotation reference. The instantaneous three-phase voltage V_k is sampled and transformed to dq components (d_s,q_s) in the bus-transformed oriented referenceframe. This transformed Line-oriented reference in the MATLAB/SIMULINK model block: abc to dq0, dq0 to abc model block are used for this transformation. The block is formed in the MATLAB/SIMULINK control and measurements/transformation library.

The Switching Logic (Pulse Generator) generates the pulses that control the voltage source converters. As indicated, this is triggered by the phase shift ($\alpha \; and \; \beta$) or the modulation index (M_{sh} and M_{se}). In the implementation of the UPFC controller design, the pulse generator is implemented with the MATLAB/SIMULINK pulse generator (Thyristor). The generator for the six-pulse thyristor converter can be configured to fire the FACTS device either with ($\alpha \; and$ the or with (M_{sh} and M_{se}). The series controller operates similarly to the shunt controller, in this case adjusting the series angle.

PLACEMENT OF THE UPFC ON THE NETWORK

Optimal placement of the FACTS device is key. Optimal loss reduction can be obtained when UPFC is appropriately placed in the network. The eigenvalue, damping ratio and participation factor analyses were used to determine the most stable power system bus in the transmission line network.

RESULTS AND DISCUSSION

For the simulation, the single-line diagram of the Nigerian 330 single-line transmission network is used to create the SIMULINK digital model of the case study power system. The power system consists of 14 generators, 59 buses, 39 load points and 111

transmission lines. The case study power system is single-line MATLAB/SIMULINK. Figure 4 shows the SIMULINK model of the power system.

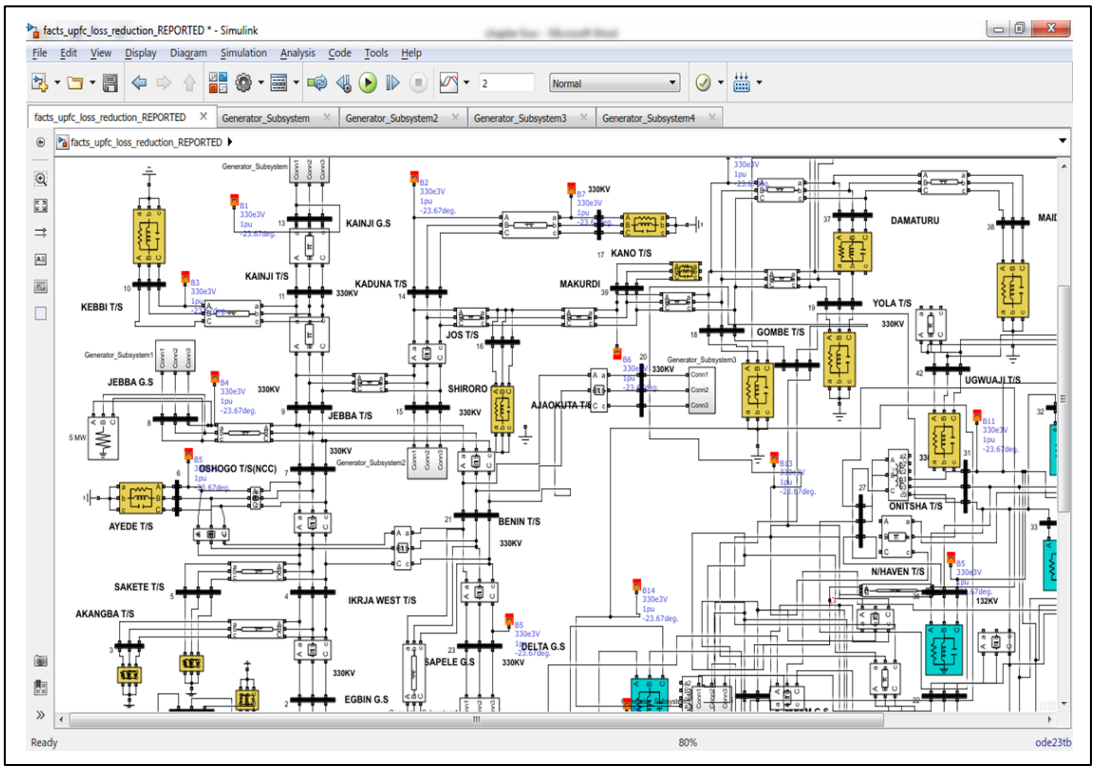


Figure 3: Simulink Model of Nigerian 330 kV Power Systems Network.

The load on a particular bus is varied and the effect of this variation is observed.The selected bus for this purpose is chosen from eigenvalue, damping ratio and participation factor analyses. Table 1 illustrates the outcome of the analyses carried out on the controlled network.

Table 1. Extracted output from eigenvalue, damping ratio and participation factor analyses on the modelled network.

Bus No.	Bus	Eigenvalue(λ)	Damping ratio(G)	PartEigenvalueactor (%)
1	Lekki T/S	-04164±j0.6618	0.4762	0.0102
2	Alagbon T/S	-2.325±j8.0321	0.2781	2.0018
3	Aja T/S	-5.6837±j10.3601	0.4810	0.2146
4	Okearo T/S	2.4892±j10.8650	0.2233	10.1575
5	Egbin G/S	-0.4087±j0.8293	0.4421	0.0625
6	Akangba T/S	0.8922±j3.013	0.2842	3.1174
7	Ikeja west T/S	-5.3063±j10.3295	0.4569	0.0625

8	Sakete T/S	-5.1617±j11.2755	0.4162	12.4678
9	Omotosho (NIPP)	-0.4759±j0.5616	0.6465	0.0933
10	Olorunsogo G/S	-04164±j0.6618	0.5325	0.0536
11	Ayede T/S	2.0922±j7.914	0.2562	2.0341
12	Oshogbo T/S	-1.1731±j4.1051	0.2751	4.3210
13	Jebba T/S	-0.8042±j2.9632	0.2623	0.7326
14	Jebba G/S	-1.1843±j3.845	0.2942	3.0072
15	Kebbi T/S	-1.1012±j3.1752	0.3283	0.4136
16	Kainji T/S	-0.9499±j3.5917	0.2552	2.0018
17	Kaduna T/S	-4.0428±j5.80451	0.5716	1.4172
18	Jos T/S	5.5160±j5.22030	0.7108	8.3066
19	Kano T/S	-3.7688±j6.0058	0.5315	3.4172
20	Makurdi T/S	-3.2505±j82795	0.36543	0.9847
21	Gombe T/S	-2.8394±j7.8648	0.3396	2.6731
22	Damaturu T/S	2.6431±j8.0318	0.3126	0.9874
23	Maiduguri T/S	-2.9202±j7.7275	0.3536	0.0378
24	Yola T/S	3.5157±j6.3330	0.4762	0.0102
25	Ganmo T/S	-2.325±j8.03211	0.3781	1.0018
26	Shiroro G/S	-5.6837±j10.3601	0.2810	0.2146
27	Katampe T/S	-2.4892±j10.8650	0.2233	0.1575
28	Gwagwalada T/S	-2.4087±j0.8293	0.5421	0.0625
29	Lokoja T/S	-0.8922±j3.0136	0.2842	5.1174
30	Ajaokuta T/S	3.3063±j12.3295	0.3569	0.0625
31	Geregu G/S	-5.1617±j11.275	0.4162	2.4678
32	Ihovbor NIPP	-0.4759±j0.5616	0.3465	2.0933
33	Benin T/S	-04164±j0.6618	0.5325	0.0536
34	Delta G/S	-2.0922±j7.9144	0.2562	2.0341
35	Sapele NIPP	-1.1731±j4.1051	0.2751	4.3210
36	Aladja T/S	-0.8042±j2.9632	0.2623	0.7326
37	Asaba T/S	1.1343±j3.3456	0.2942	1.0072
38	Alaoji G/S	-1.1012±j3.1752	0.3283	0.4136
39	Owerri T/S	-0.9499±j3.5917	0.2552	2.0018
40	Alaoji T/S	-3.0428±j5.80451	0.5716	1.4172
41	Onitsha T/S	5.5160±j5.22030	0.3108	5.3066
42	Okpai G/S	-3.7688±j6.0058	0.5315	3.4172
43	N. Haven T/S	-2.2505±j82795	0.3654	1.9847
44	Ugwuaji T/S	-2.8394±j7.8648	0.3396	2.6731

45	Ikot-Ekpene T/S	-1.6431±j8.0318	0.3126	2.9874
46	Odukpani G/S	-2.9202±j7.7275	0.2536	1.0378
47	Adiabor T/S	-5.5957±j10.333	0.3762	0.0102
48	Ibom G/S	-2.325±j8.03211	0.2781	3.0018
49	Eket T/S	-5.6837±j10.360	0.8810	2.2146
50	Itu T/S	-2.4892±j10.865	0.2233	4.1575
51	P/H main T/S	-3.4087±j0.8293	0.4421	0.0625
52	Yenagoa T/S	-0.8922±j3.0135	0.2842	3.1174
53	Omoku G/S	-5.3063±j4.3295	0.4569	0.0625
54	Transamadi G/S	-3.1617±j1.2755	0.4162	6.4678
55	Rivers IPP G/S	0.4759±j0.5616	0.6465	0.0933
56	AES G/S	-04164±j0.6618	0.5325	0.0536
57	Gbarain G/S	-2.0922±j7.914	0.2562	2.0341
58	Ahaoda T/S	-6.1731±j4.1051	0.2751	4.3210
59	ASCO G/S	-0.8042±j2.9632	0.2623	0.7326

The eigenvalue (λ) gives information about the status of the system to stability. The bus participation factor shows the weak zones of the system. The damping ratio (ς) is an indication of the ability of the system to return to a stable state in the event ofsystem disturbances. From Table 1, it can be noticed that the real part of the complex eigenvalue is not all negative. This means they are not all placed on the left side (i.e. the stable location) of the s-plane. This means the system is not in stable conditions. The real part of the eigenvalue in the left–half of the s-plane defines an exponentially decaying component in the system. Values far from the origin to the left-hand of the s-plane correspond to stable components, while values near the origin correspond to slowly decaying components. However, not all the buses in the power system contribute to system instability. From Table 1, most of the eigenvalues are located on the left side of the S- plane. Among the buses whose eigenvalues were located on the left side of the S- plane, the most stable bus was selected for load variation for the evaluation of the loss reduction. Since one bus is to be selected, the damping ratio was used as the criteria for the selection. The higher the damping ratio, the more stable the bus. The bus with a negative eigenvalue and the highest damping ratio was selected. The selected bus was subjected to load variation. Whereas loads at other buses were held constant at the demand values. From Table 1, the bus selected was Eket T/S. The eigenvalue and damping ratio of this bus was -5.6837±j10.3601 and 0.8810 respectively.The variation of load on the bus began at 198 MW with an increment of 50 % (i.e. 99MW). Hence, the variations of loading conditions at the bus are 198 MW, 297 MW, 396 MW, 495 M, and 594 MW.Table 2 shows the losses (real and reactive)

obtained from the load flow study of the network with load variation drawn at Eket T/S with and without UPFC.

Table 2. Power losses with load variation in the power system with and without UPFC installed

	Total active power loss(p.u)		Total Reactive power loss(p.u)	
Load variation(MW)	**Without UPFC**	**With UPFC**	**Without UPFC**	**With UPFC**
198	11.1730	7.8838	60.7648	55.8455
297	12.1387	10.7512	68.4904	59.7880
396	13.1044	11.5169	84.1944	64.7305
495	13.8587	12.4826	97.1322	66.6730
594	14.7901	13.4483	113.3895	73.6155

The overall system loss was reduced with the installation of Neural Network controlled UPFC as seen in Table 2.
Table 3 shows the transmission lines in the modelled power systems network.

Table 3. Transmission Lines [1]

From bus	To bus	Line#
KEBBI	KAINJI GS	1
GANMO	JEBBA TS	2
YENEGOA	GBARAIN	3
EKET 132KV	IBOM 132KV	4
EKET 132KV	IBOM 132KV	5
ITU 132KV	EKET 132KV	6
ABA 132KV	ITU 132KV	7
KADUNA	SHIRORO	8
JEBBA TS	SHIRORO	9
KADUNA	JOS	10
GANMO	OSHOBO	11
AYEDE	OLORUNSOGO TS	12
IHOVBOR TS	BENIN	13
OKEARO TS	EGBIN TS	14
ONITSHA	ALAOJI 330KV	15
OSHOBO	IHOVBOR TS	16
UGWUAJI	NEW HEAVEN	17

OLORUNSOGO TS	OLORUNSOGO GS	18
OLORUNSOGO TS	IKEJA WEST	19
SHIRORO	GWAGWA	20
SAKETE	IKEJA WEST	21
GOMBE	JOS	22
AKANGBA	IKEJA WEST	23
SAPELLE	ALADJA	24
OKEARO TS	EGBIN TS	25
IKEJA WEST	EGBIN TS	26
OMOTOSO TS	BENIN	27
EGBIN TS	EGBIN GS	28
OMOTOSO GS	OMOTOSO TS	29
LEKKI	AJA	30
BENIN	DELTA	31
BENIN	ONITSHA	32
LEKKI	ALAGBON	33
ONITSHA	NEW HEAVEN	34
EGBIN TS	AJA	35
UGWUAJI	IKOT EKPENE	36
AJAOKUTA	BENIN	37
BENIN	SAPELLE	38
JOS	MAKURDI	39
EGBIN TS	AJA	40
IKEJA WEST	OMOTOSO TS	41
DELTA	ALADJA	42
AFAM	AFAM GS	43
AJA	ALAGBON	44
KADUNA	KANO	45
KATAMPE	GWAGWA	46
SHIRORO	KATAMPE	47
GWAGWA	LOKOJA	48
AJAOKUTA	LOKOJA	49
JEBBA TS	KAINJI GS	50
BENIN	ONITSHA	51
SHIRORO GS	SHIRORO	52
AJAOKUTA	GEREGU GS	53
EGBIN TS	BENIN	54
AJAOKUTA	BENIN	55

ONITSHA	OKPAI GS	56
BENIN	ASABA	57
ASABA	ONITSHA	58
IKOT EKPENE	ODUKPANI G.S	59
ONITSHA	OKPAI GS	60
OSHOBO	AYEDE	61
MAKURDI	UGWUAJI	62
UGWUAJI	IKOT EKPENE	63
ALAOJI 330kV	IKOT EKPENE	64
ALAOJI 330kV	AFAM	65
ODUKPANI G.S	ADIABOR	66
ODUKPANI G.S	ADIABOR	67
ALAOJI 330kV	ALAOJI GS	68
DAMATURU	GOMBE	69
IKORODU	SAGAMU	70
AKANGBA	IKEJA WEST	71
YOLA	GOMBE	72
IKEJA WEST	OKEARO TS	73
IKEJA WEST	OKEARO TS	74
JEBBA TS	OSHOBO	75
JEBBA TS	KAINJI GS	76
JEBBA TS	SHIRORO	77
KADUNA	SHIRORO	78
MAKURDI	UGWUAJI	79
JOS	MAKURDI	80
JEBBA GS	JEBBA TS	81
DAMATURU	MAIDUGURI	82
OSHOBO	IKEJA WEST	83
SHIRORO	GWAGWA	84
AJAOKUTA	LOKOJA	85
UGWUAJI	NEW HEAVEN	86
UGWUAJI	IKOT EKPENE	87
UGWUAJI	IKOT EKPENE	88
ALAOJI 330kV	IKOT EKPENE	89
RIVERS 132kV	AFAM 132kV	90
RIVERS 132kV	AFAM 132kV	91
IKOT EKPENE	ODUKPANI G.S	92
OWERRI	ALAOJI 132kV	93

JEBBA TS	OSHOBO	94
OWERRI	ALAOJI 132kV	95
OWERRI	AHOADA	96
OWERRI	AHOADA	97
AHOADA	OMOKU	98
AHOADA	OMOKU	99
PH MAINS	RIVERS 132kV	100
PH MAINS	RIVERS 132kV	101
YENEGOA	AHOADA	102
YENEGOA	AHOADA	103
YENEGOA	GBARAIN	104
EGBIN TS	IKORODU	105
AFAM	AFAM 132kV	106
AFAM	AFAM 132kV	107
ALAOJI 330kV	ABA 132kV	108
ADIABOR	ITU 132kV	109
ALAOJI 330kV	ALAOJI 132kV	110
ALAOJI 330kV	ALAOJI 132kV	111

Figures 5, 6, 7, 8, 10, 11, 12, 13 and 14 show the plot for the active and reactive power losses in the transmission lines for the power system with and without the UPFC installed for the 198 MW, 297 MW, 396 MW, 495 MW and 594 MW loads respectively.

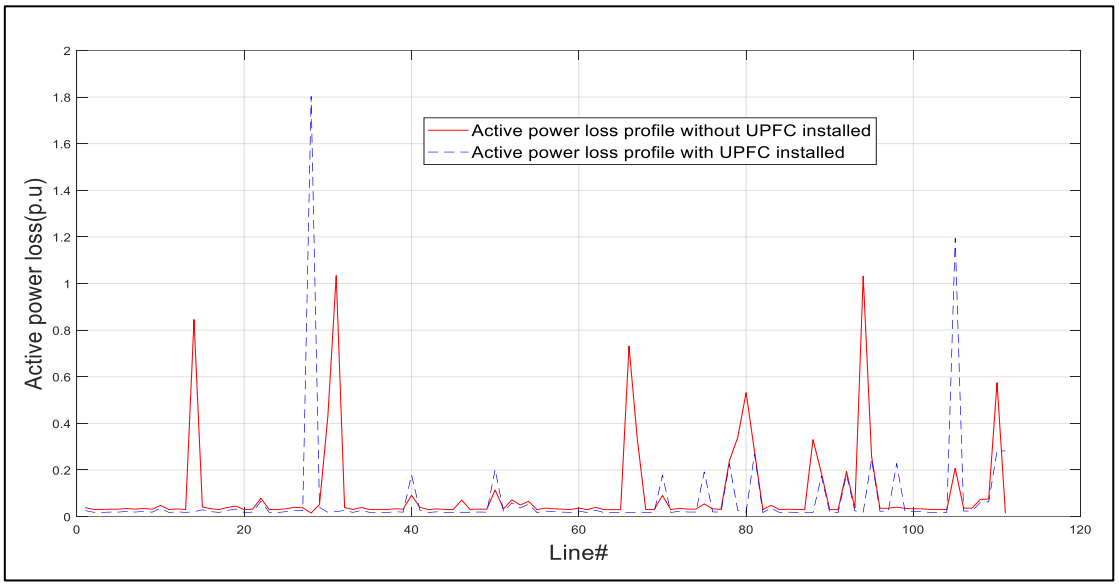


Figure 5. Comparison of active power loss distribution in the power system with and without UPFC installed for the 198 MW load drawn at Eket T/S

From Figure 5, it can be observed that the active loss without the UPFC installed is higher than with the UPFC installed. However, the distribution of the levels of losses in certain lines deviated from the expected outcome. Key examples can be seen in lines 28 and 105. This was because of the complexities and nonlinearity of the power system. Despite these deviations, the overall system loss was reduced with the installation of UPFC as seen in Table 2.

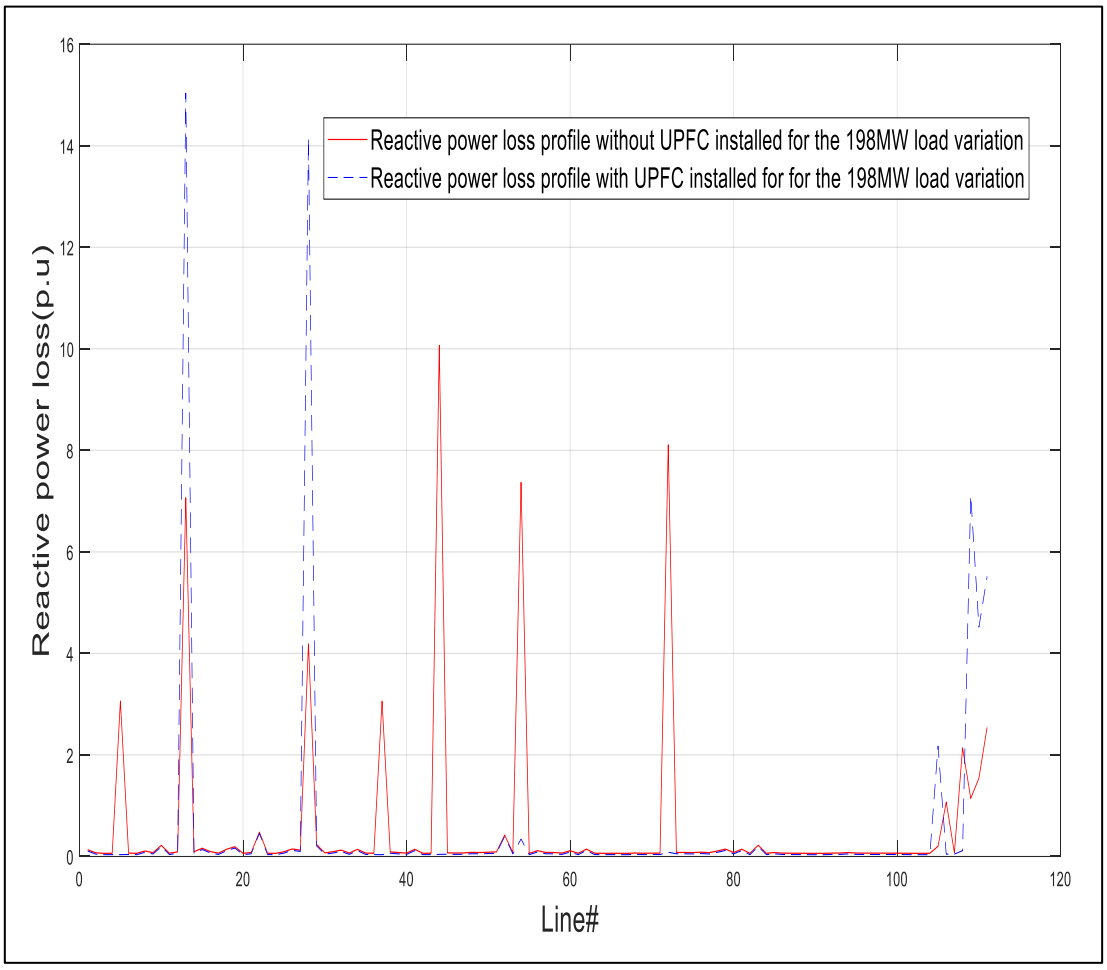


Figure 6. Comparison of reactive power loss distribution in the power system with and without UPFC installed for the 198MW load drawn**.**

From Figure 6, it can be observed that the reactive power loss without the UPFC installed is higher than with the UPFC installed. However, the distribution of the levels of losses in certain lines deviated from the expected outcome. Key examples can be seen in lines 13, 28, 104 and 111. This was because of the complexities and nonlinearity of the power system. Despite these deviations, the overall system loss was reduced with the installation of UPFC as seen in Table 2.

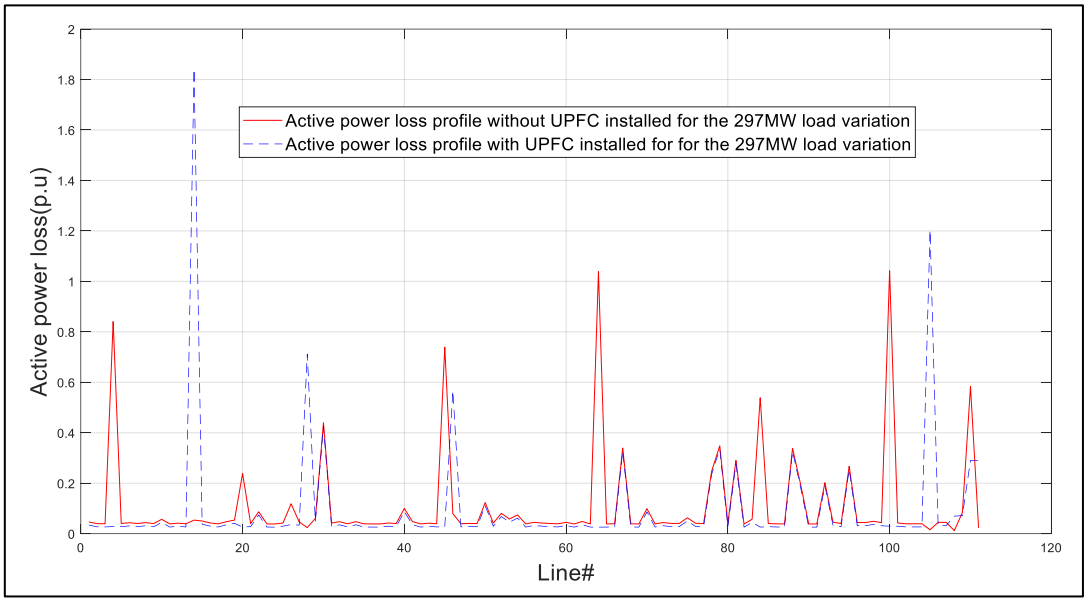


Figure 7. Comparison of active power loss distribution in the power system with and without UPFC installed for the 297 MW load drawn

From Figure 7, it can be observed that the active power loss without the UPFC installed is higher than with the UPFC installed. However, the distribution of the levels of losses in certain lines deviated from the expected outcome. Key examples can be seen inlines 14, 28, 46 and 105. This was because of the complexities and nonlinearity of the power system. Despite these deviations, the overall system loss was reduced with the installation of UPFC as seen in Table 2.

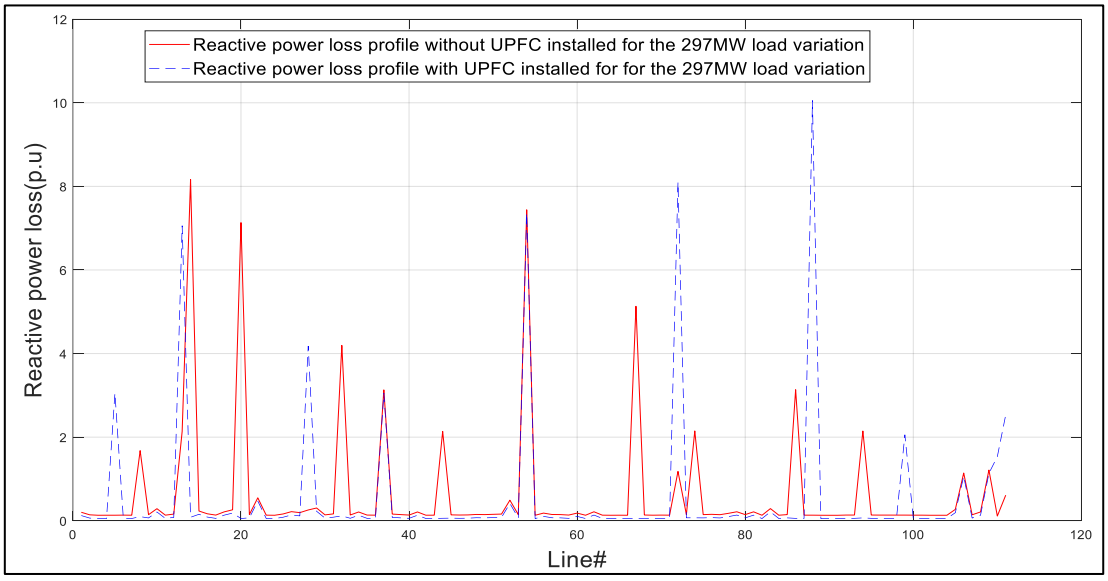


Figure 8. Comparison of reactive power loss distribution in the power system with and without UPFC installed for the 297 MW load drawn

From Figure 8, it can be observed that the reactive power loss without the UPFC installed is higher than with the UPFC installed. However, the distribution of the levels of losses in certain lines deviated from the expected outcome. Key examples can be seen in lines 5, 28, 72, 88, 99 and 111. This was because of the complexities and nonlinearity of the power system. Despite these deviations, the overall system loss was reduced with the installation of UPFC as seen in Table 2.

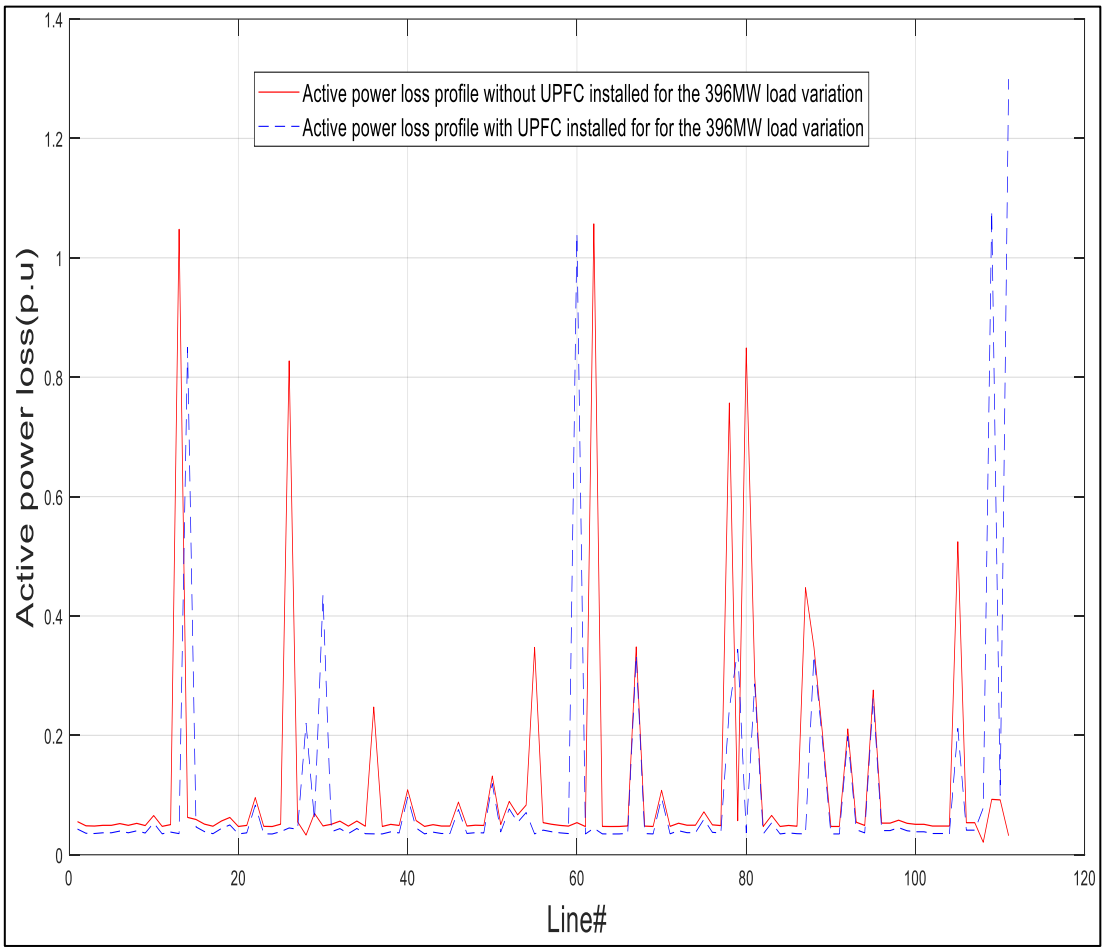


Figure 9. Comparison of active power loss distribution in the power system with and without UPFC installed for the 396 MW load drawn

From Figure 9, it can be observed that the active power loss without the UPFC installed is higher than with the UPFC installed. However, the distribution of the levels of losses in certain lines deviated from the expected outcome. Key examples can be seen in lines 14, 30, 60, 79, 109 and 111. This was because of the complexities and nonlinearity of the power system. Despite these deviations, the overall system loss was reduced with the installation of UPFC as seen in Table 2.

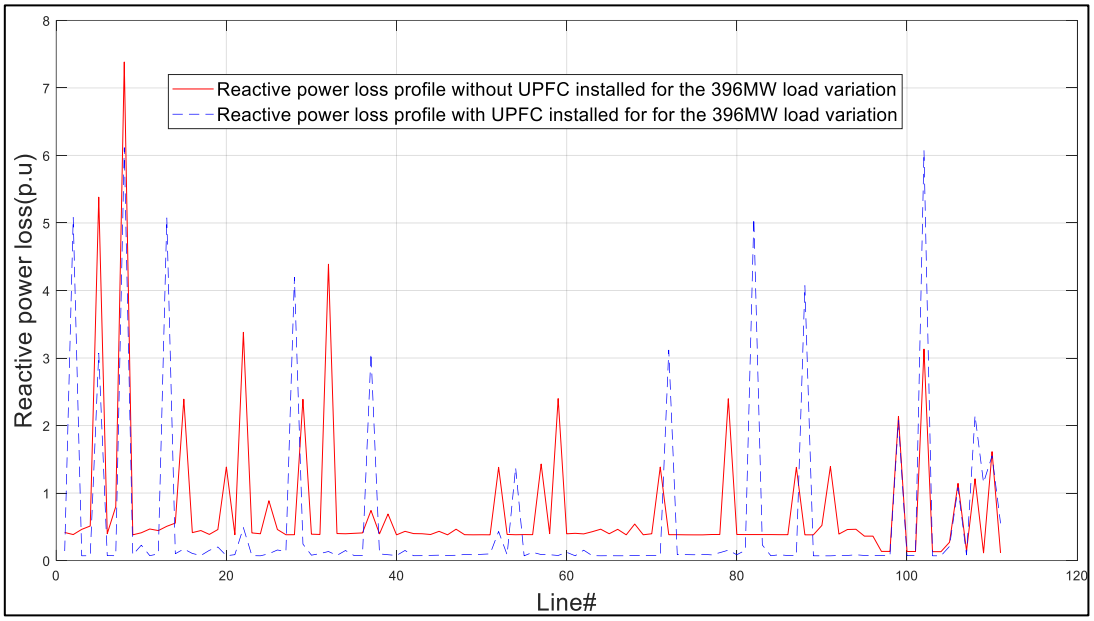


Figure 10. Comparison of reactive power loss distribution in the power system with and without UPFC installed for the 396 MW load drawn

From Figure 10, it can be observed that the reactive power loss without the UPFC installed is higher than with the UPFC installed. However, the distribution of the levels of losses in certain lines deviated from the expected outcome. Key examples can be seen in lines 2, 13, 28, 37, 54, 72, 82, 102 and 108. This was because of the complexities and nonlinearity of the power system. Despite these deviations, the overall system loss was reduced with the installation of UPFC as seen in Table 2.

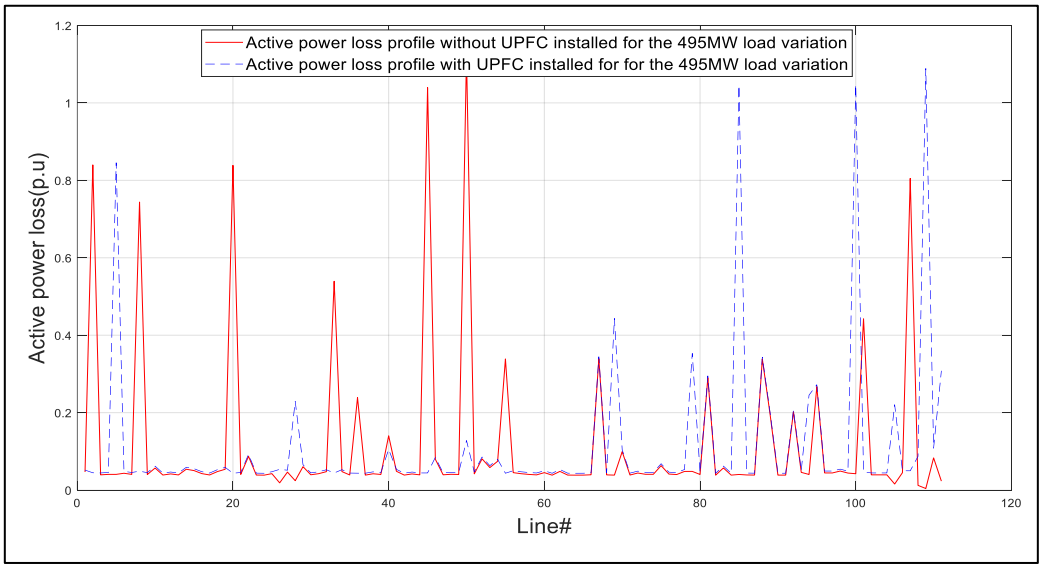


Figure 11. Comparison of active power loss distribution in the power system with and without UPFC installed for the 495 MW load drawn

From Figure 11, it can be observed that the active power loss without the UPFC installed is higher than with the UPFC installed. However, the distribution of the levels of losses in certain lines deviated from the expected outcome. Key examples can be seen in lines 5, 28, 69, 79, 85, 100, 109 and 110. This was because of the complexities and nonlinearity of the power system. Despite these deviations, the overall system loss was reduced with the installation of UPFC as seen in Table 2.

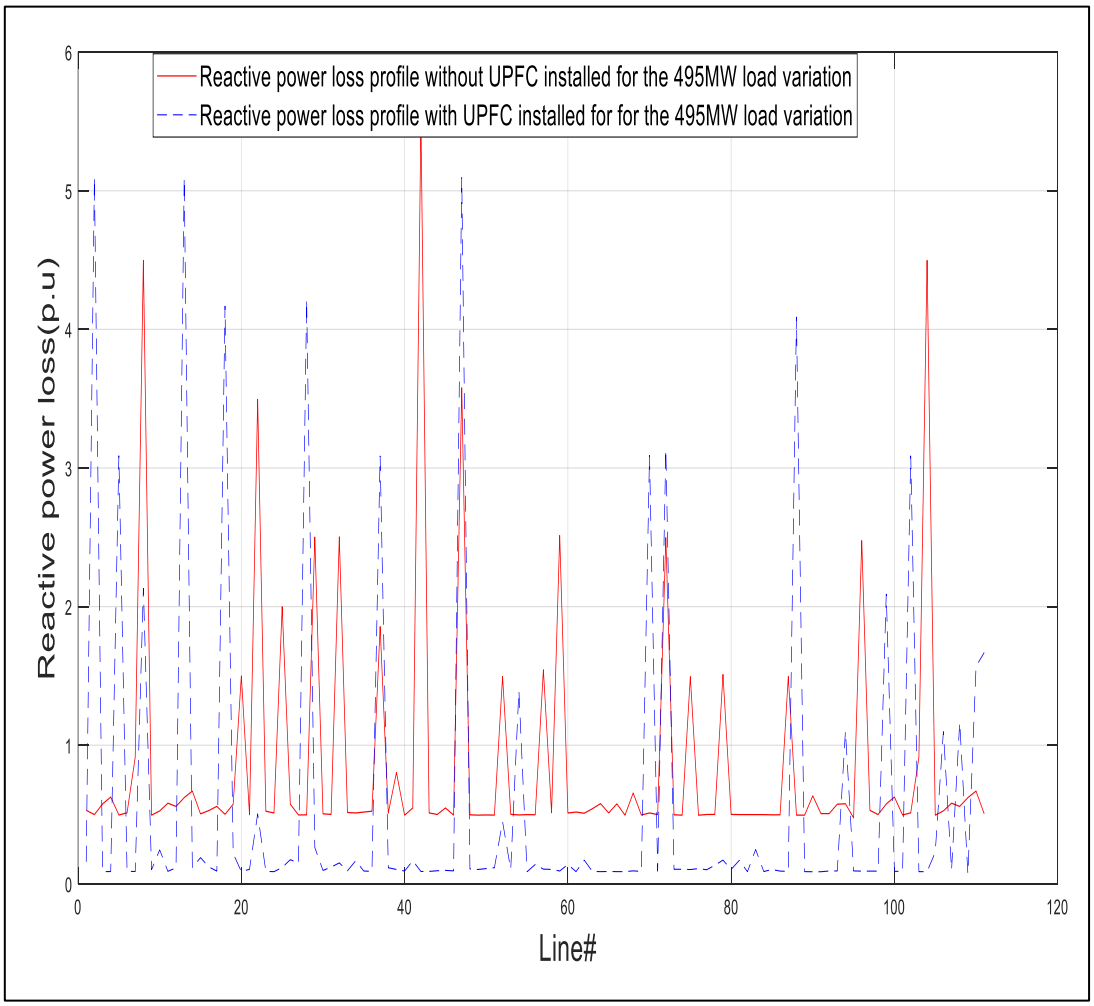


Figure 12. Comparison of reactive power loss distribution in the power system with and without UPFC installed for the 495 MW load drawn

From Figure 12, it can be observed that the reactive power loss without the UPFC installed is higher than with the UPFC installed. However, the distribution of the levels of losses in certain lines deviated from the expected outcome. This was because of the complexities and nonlinearity of the power system. Despite these deviations, the overall system loss was reduced with the installation of UPFC as seen in Table 2.

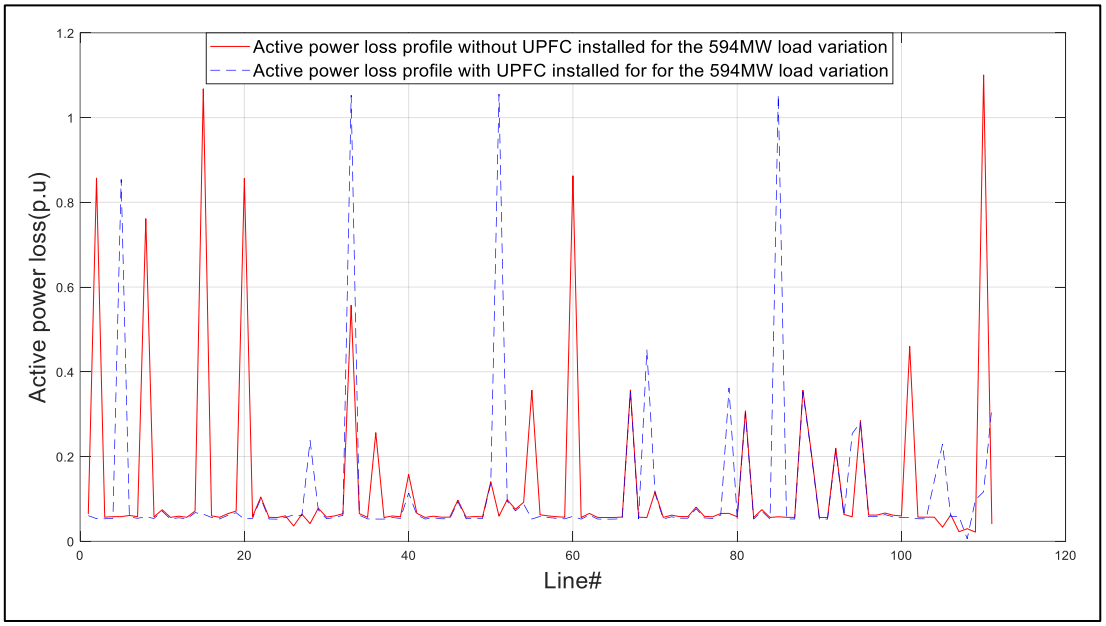


Figure 13. Comparison of active power loss distribution in the power system with and without UPFC installed for the 594 MW load drawn

From Figure 13, it can be observed that the active power loss without the UPFC installed is higher than with the UPFC installed. However, the distribution of the levels of losses in certain lines deviated from the expected outcome. Key examples can be seen in lines 5, 28, 33, 51, 69, 79, 84 and 105. This was because of the complexities and nonlinearity of the power system. Despite these deviations, the overall system loss was reduced with the installation of UPFC as seen in Table 2.

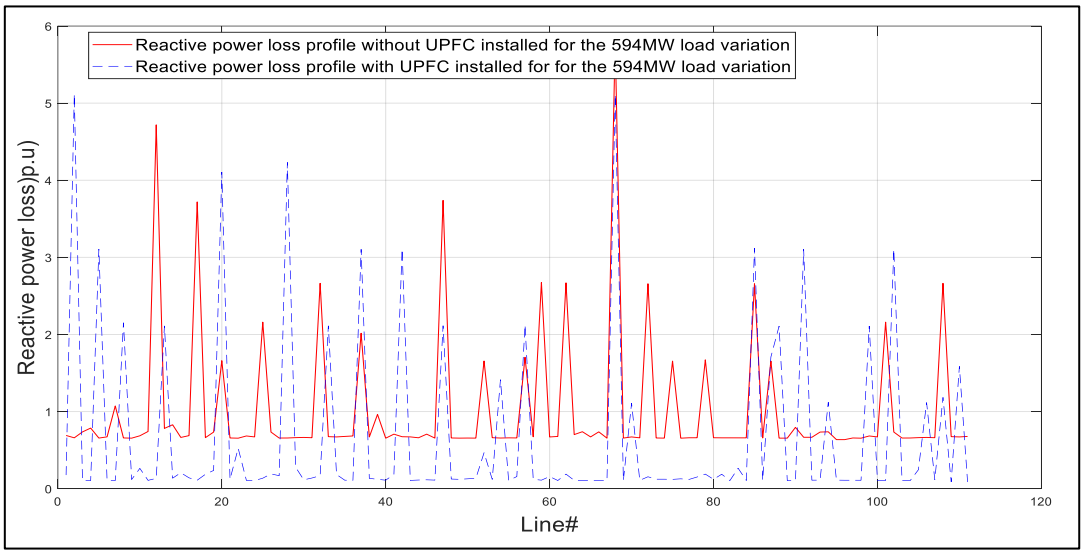


Figure 14. Comparison of reactive power loss distribution in the power system with and without UPFC installed for the 594 MW load drawn

From Figure 14, it can be observed that the reactive power loss without the UPFC installed is higher than with the UPFC installed. However, the distribution of the levels of losses in certain lines deviated from the expected outcome. Key examples can be seen in lines 2, 5, 8, 13, 20, 28, 33, 37, 41, 47, 54, 57, 70, 85, 88, 91, 94, 99, 102 and 110. This was because of the complexities and nonlinearity of the power system. Despite these deviations, the overall system loss was reduced with the installation of UPFC as seen in Table 2.

The system loss was also obtained with the installation of a Thyristor Controlled Series Capacitor (TCSC). The result obtained was compared with that obtained for UPFC and represented in Table 4.

Table 4. Comparison of active and reactive loss reduction for load variations with FACTS devices installed in the power systems network.

	Active power loss(P.U)			Reactive power loss(P.U)			Active power loss reduction (%)		Reactive power loss reduction (%)	
Load variation (MW)	**Without FACTS**	**With TCSC**	**With UPFC**	**Without FACTS**	**With TCSC**	**With UPFC**	**With TCSC**	**With UPFC**	**With TCSC**	**With UPFC**
198	11.1730	9.5191	7.8838	60.7648	58.8223	55.8455	14.8026	29.44	3.1967	8.10
297	12.1387	11.1730	10.7512	68.4904	64.8940	59.7880	7.9555	11.43	5.2509	27.71
396	13.1044	12.2386	11.5169	84.1944	77.8341	64.7305	6.6069	12.15	7.5543	23.12
495	13.8587	13.3138	12.4826	97.1322	85.5993	66.6730	3.9318	9.93	11.8734	31.36
594	14.7901	13.8244	13.4483	113.3895	98.1942	73.6155	6.5293	9.07	13.4009	33.08
Average Value (%)	**13.01**	**12.01**	**11.22**	**84.794**	**77.07**	**64.130**	**7.965**	**14.404**	**8.255**	**24.67**

The overall system loss was reduced with the installation of Neural Network controlled UPFC as seen in Table 4.

CONCLUSION

The electrical energy is produced and transmitted to load centres. As a result of the physical properties of the transmission medium, some of the transmitted powers are lost to the surroundings. The overall effect of power losses on the system is a reduction in the quantity of power available to the consumers. Power loss leads to the high cost of power generation, transmission and distribution.

In this work neural network-controlled UPFC was used for the reduction of losses in power transmission networks. In the modelling of the neural network controller for the UPFC, the input parameters of the neural controller include power system variables that relate to the control of ohmic and corona losses on transmission lines.

The Nigerian 330kV power grid was used as a case study for the evaluation of the proposed power loss reduction system. The digital model of the case study power system with the proposed neural network controlled UPFC integrated was created in the MATLAB/SIMULINK programming environment.

The simulation carried out involved the alteration of power flow to cause different levels and distribution of losses in the network. With each variation, load flow studies were done to evaluate the distribution of losses and the active and reactive loss reduction achieved by the proposed system. The simulation and evaluations are carried out under two scenarios: (i) with the UPFC installed and (ii) without the UPFC installed. With each variation of load at the bus, load flow is run to determine total system loss either with the UPFC installed or without the UPFC installed.

Results obtained showed that the proposed system achieved an average active power loss reduction of 14.40% and an average reactive power loss reduction of 24.67%. The performance of the proposed system was compared with that of the TCSC. Findings showed that the proposed neural network-controlled UPFC achieved better active and reactive power loss reduction than the TCSC. It outperformed the TCSC by 6.08 % in the reduction of active loss and by 15.345% in the reduction of reactive power loss in the power system.

ACKNOWLEDGEMENT

I humbly wish to acknowledge the management of Abia State Polytechnic, Aba for giving me an enabling ground to carry out this research work on record time and also the federal ministry of education through the Tertiary Education Trust Fund (TETFUND) for the research grant award that enabled me in actualizing the desired result of the research work in my field of study effectively.

REFERENCES

[1] C. Chiatula, D. I. Chinda, R. Onoshakpor and S. Abba-Aliyu, "Utilisation of FACTS devices in the Nigerian transmission grid," in *IEEE PES/IAS Power Africa*, Virtual Event, 2020 .

[2] O. Bamigbola, M. Ali and M. Oke, "Mathematical modelling of electric power flow and the minimization of power losses on transmission lines," *Applied Mathematics and Computation,* vol. 3, no. 2, pp. 214-221, 2014.

[3] B. Bhattacharyya and S. Kumar, "Loadability enhancement with FACTS devices using gravitational search algorithm," *International Journal of Electrical Power and Energy Systems (ELSEVIER),* vol. 78, pp. 470-479, 2016.

[4] A. I. Onyegbadue and T. C. Madueme, "Theoretical Aspects of Optimization Using FACTS Devices," *International Journal of Engineering Research & Technology,* vol. 3, no. 10, pp. 632-635, 2015.

[5] D. Gaur and L. Mathew, "Optimal placement of FACTS devices using optimization techniques: A review," in *IOP Conference series: materials science and engineering*, BKBIET Pilani , 2018.

[6] T. C. Madueme and I. A. Onyegbadue, "Application of UPFC for Optimization of the Nigeria Electric Power System," *International Journal of Engineering and Emerging Scientific Discovery,* vol. 3, no. 2, pp. 82-94, 2018.

[7] B. Bhattacharyya and S. Kumar, "Approach for the solution of transmission congestion with multi-type FACTS devices," *IET Generation, Transmission and Distribution,* vol. 10, no. 11, pp. 2802-2809, 2016.

[8] M. M. Ibrahim, J. Jahin Al Hasan, M. R. Islam, H. Nayeema, M. A.-S. Ubaid, H. M. Ahmad, I. I. Ahmed, A. Abdullah, R. Muhyaddin and B. Hussain, "Reducing Fault Current by Using FACTS Devices to Improve Electrical Power Flow," *Mathematical Problems in Engineering (HINDAWI),* vol. 2021, pp. 1-9, 2021.

[9] H. M. Daealhaq, Y. F. key and A. S. Tukkee, "Power loss reduction and voltage profile improvement using optimal placement of FACTS devices," in *4th IOP Conference Series: Materials Science and Engineering*, Kerbala Iraq, 2021.

[10] M. H. Ananda and M. R. Shivakumar, "An Overview of UPFC with PSS for Power Flow Control and System Stability," *International Journal of Applied Engineering Research,* vol. 13, no. 22, pp. 15701-15707, 2018.

[11] O. I. Abiodun, A. Jantan, A. E. Omolara, K. V. Dada, N. A. Mohamed and H. Arshad, "State-of-the-art in artificial neural network applications: A survey," *Heliyon,* vol. 4, no. 11, pp. 1- 41, 2018.

[12] S. Chapaloglou, A. Nesiadis, P. Iliadis, K. Atsonios, N. Nikolopoulos, P. Grammelis, C. Yiakopoulos, I. Antoniadis and E. Kakaras, "Smart energy management algorithm for load smoothing and peak shaving based on load forecasting of an island's power system," *Applied Energy,* vol. 238, pp. 627- 642, 2019.

[13] A. T. Hoang, S. Niveti, H. C. Ong, W. Tarelko, T. H. Le, M. Q. Chau and X. P. Nguyen, "A review on application of artificial neural network (ANN) for performance and emission characteristics of a diesel engine fueled with biodiesel-based fuels," *Sustainable Energy Technologies and Assessments (Elsevier),* vol. 47, no. 2, pp. 1-21, 2021.

[14] P. Sekhar and S. Mohanty, "An online power system static security assessment module using multi-layer perceptron and radial basis function network," *International Journal of Electrical Power and Energy Systems,* vol. 76, no. 3, pp. 165-173, 2016.

[15] K. Teeparthi and D. Vinod Kumar, "Power System Security Assessment and Enhancement: A Bibliographical Survey," *Journal of The Institution of Engineers (India): Series B,* vol. 101, no. 2, pp. 163-176, 2020.

[16] S. Liu, L. Liu, Y. Fan, L. Zhang, Y. Huang, T. Zhang, J. Cheng, L. Wang, M. Zhang and R. Shi, "An integrated scheme for online dynamic security assessment based on partial mutual information and iterated random forest," *IEEE Transactions on Smart Grid,* vol. 11, no. 4, pp. 3606-3619, 2020.

[17] V. Veerasamy, N. I. A. Wahab, R. Ramachandran, M. L. Othman, H. Hizam, V. S. Devendran, A. X. R. Irudayaraj and A. Vinayagam, "Recurrent network based power flow solution for voltage stability assessment and improvement with distributed energy sources," *Applied Energy,* vol. 302, p. 117524, 2021.

[18] M. Amin and M. Molinas, "Small-signal stability assessment of power electronics based power systems: A discussion of impedance-and eigenvalue-based methods," *IEEE Transactions on Industry Applications,* vol. 53, no. 5, pp. 5014-5030, 2017.

[19] F. M. Albatsh, S. Mekhilef, S. Ahmad and H. Mokhlis, "Fuzzy-logic-based UPFC and laboratory prototype validation for dynamic power flow control in transmission lines," *IEEE Transactions on Industrial Electronics,* vol. 64, no. 12, pp. 9538-9548, 2017.

[20] P. De Rua, C. S. Özgür and B. Jef, "Comparative study of dynamic phasor and harmonic state-space modelling for small-signal stability analysis," *Electric Power Systems Research,* vol. 189, pp. 106-112, 2020.

[21] J. Lyu, X. Zhang, X. Cai and M. Molinas, "Harmonic state-space based small-signal impedance modelling of a modular multilevel converter with consideration of internal harmonic dynamics," *IEEE Transactions on Power Electronics,* vol. 34, no. 3, pp. 2134-2148, 2018.

[22] Y. Liao, Z. Liu, H. Zhang and B. Wen, "Low-frequency stability analysis of single-phase system with dq frame impedance approach—Part II: Stability and frequency analysis," *IEEE Transactions on Industry Applications,* vol. 54, no. 5, pp. 5012-5024, 2018.

[23] X. Wang and F. Blaabjerg, "Harmonic stability in power electronic-based power systems: Concept, modelling, and analysis," *IEEE Transactions on Smart Grid,* vol. 10, no. 3, pp. 2858-2870, 2018.

[24] M. Begum, L. Li, J. Zhu and Z. Li, "State-space modelling and stability analysis for microgrids with distributed secondary control," in *2018 IEEE 27th International Symposium on Industrial Electronics (ISIE)*, Cairns, Australia, 2018.

[25] D. Xie, Y. Lu, J. Sun and C. Gu, "Small signal stability analysis for different types of PMSGs connected to the grid," *Renewable Energy,* vol. 106, pp. 149-164, 2017.

[26] E. Ebrahimzadeh, F. Blaabjerg, X. Wang and C. L. Bak, "Bus participation factor analysis for harmonic instability in power electronics based power systems," *IEEE Transactions on Power Electronics,* vol. 33, no. 12, pp. 10341-10351, 2018.

[27] H. Hu, H. Tao, X. Wang, F. Blaabjerg, Z. He and S. Gao, "Train-network interactions and stability evaluation in high-speed railways—Part II: Influential factors and verifications," *IEEE Transactions on Power Electronics,* vol. 33, no. 6, pp. 4643-4659, 2017.

[28] A. Al-Awami, Y. L. Abdel-Magid and M. A. Abido, "Simultaneous stabilization of power system using UPFC-based controllers," *Electric Power Components and Systems,* vol. 34 no. 9, pp. 941-959, 2006.